A Structural Study of GDP-4-Keto-6-Deoxy-D-Mannose-3-Dehydratase: Caught in the Act of Geminal Diamine Formation[†,‡]

Paul D. Cook and Hazel M. Holden*

Department of Biochemistry, University of Wisconsin, Madison, Wisconsin 53706

Received August 20, 2007; Revised Manuscript Received September 25, 2007

ABSTRACT: Di- and trideoxysugars are an important class of carbohydrates synthesized by certain plants, fungi, and bacteria. Colitose, for example, is a 3,6-dideoxysugar found in the O-antigens of Gram-negative bacteria such as *Escherichia coli*, *Salmonella enterica*, *Yersinia pseudotuberculosis*, and *Vibrio cholerae*, among others. These types of dideoxysugars are thought to serve as antigenic determinants and to play key roles in bacterial defense and survival. Four enzymes are required for the biochemical synthesis of colitose starting from mannose-1-phosphate. The focus of this investigation, GDP-4-keto-6-deoxy-D-mannose-3-dehydratase (ColD), catalyzes the third step in the pathway, namely the PLP-dependent removal of the C3′-hydroxyl group from GDP-4-keto-6-deoxymannose. Whereas most PLP-dependent enzymes contain an active site lysine, ColD utilizes a histidine as its catalytic acid/base. The ping-pong mechanism of the enzyme first involves the conversion of PLP to PMP followed by the dehydration step. Here we present the three-dimensional structure of a site-directed mutant form of ColD whereby the active site histidine has been replaced with a lysine. The electron density reveals that the geminal diamine, a tetrahedral intermediate in the formation of PMP from PLP, has been trapped within the active site region. Functional assays further demonstrate that this mutant form of ColD cannot catalyze the dehydration reaction.

Di- and trideoxysugars are an intriguing class of carbohydrates that are synthesized by plants, fungi, and bacteria (*1*, *2*). The biosynthetic pathways for the production of these unusual sugars typically begin with simple monosaccharides such as glucose-1-phosphate or fructose-6-phosphate as starting materials. Via an impressive array of reactions including dehydrations, reductions, amino transfers, and methylations, the pathways result in an astonishing array of sugars with differing three-dimensional shapes and hydrophilicities. Many of these unusual sugars have been isolated from the O-antigens of a variety of Gram-negative bacteria, where they contribute to the structural variations observed in bacterial cell walls (*3*). It has been suggested that these sugars play a role in the virulence of a given pathogen (*4*). Other deoxysugars have been found in polyketide antibiotics including erythromycin, azithromycin, and clarithromycin, where they are known to enhance the biological activities of the respective drugs (*5*).

The focus of this investigation is an enzyme involved in the biosynthesis of colitose, a 3,6-dideoxysugar found in the O-antigen of Gram-negative bacteria such as *Escherichia coli* (*6*), *Yersinia pseudotuberculosis* (*7*), *Salmonella enterica* (*8*), *Vibrio cholerae* (*9*), and in marine bacteria such as *Pseudoalteromonas tetraodonis* (*9*) *and Pseudoalteromonas carrageenovora* (*10*). The biosynthesis of the O-antigen requires nucleotide-linked sugars, which are transferred to the oligosaccharide chain by an array of glycosyltransferases. In the case of colitose, the sugar is linked to GDP.[1]

As indicated in Scheme 1, four enzymes are required for the biosynthesis of GDP-L-colitose (*11*−*13*). Recently, we reported the three-dimensional structure of GDP-4-keto-6-deoxy-D-mannose-3-dehydratase, hereafter referred to as ColD (*13*). This PLP-dependent enzyme catalyzes the removal of the C3′-hydroxyl group from the sugar ring (Scheme 1). While the overall three-dimensional architecture of ColD places it into the well-studied aspartate aminotransferase superfamily (*14*), it is rather unique in that it lacks the typically conserved active site lysine responsible for anchoring the cofactor to the protein. Instead, ColD contains a histidine residue (His 188) at the homologous position, which does not form a covalent bond with the cofactor. Interestingly, the ColD active site is markedly devoid of potential catalytic bases other than His 188, suggesting that this residue functions as the sole proton donor/acceptor in the catalytic mechanism (*13*). It is also noteworthy that ColD catalyzes the reaction using only PLP. In the syntheses of other 3,6-dideoxyhexoses, such as tyvelose, the removal of the C3′-hydroxyl group from the sugar moiety is catalyzed by enzyme complexes requiring NAD^+, FAD and [2Fe-2S] clusters for activity (*15*, *16*).

[†] This research was supported by an NIH grant (DK47814 to H.M.H.).

[‡] X-ray coordinates have been deposited in the Research Collaboratory for Structural Bioinformatics, Rutgers University, New Brunswick, NJ (accession no. 2R0T).

* To whom correspondence should be addressed. E-mail: Hazel_Holden@biochem.wisc.edu. Fax: 608-262-1319. Phone: 608-262-4988.

[1] Abbreviations: ESI, electrospray ionization; GDP, guanosine 5′-diphosphate; HEPES, *N*-2-hydroxyethylpiperazine-*N*′-2-ethanesulfonic acid; HEPPS, *N*-2-hydroxyethylpiperazine-*N*′-3-propanesulfonic acid; MES, 2-(*N*-morpholino)ethanesulfonic acid, $NADP^+$, nicotinamide adenine dinucleotide phosphate; Ni-NTA, nickel nitrilotriacetic acid; PLP, pyridoxal-5′-phosphate; PMP, pyridoxamine 5′-phosphate; TEV, tobacco etch virus; Tris, tris(hydroxymethyl)aminomethane.

10.1021/bi701686s CCC: $37.00
Published on Web 11/13/2007

Scheme 1

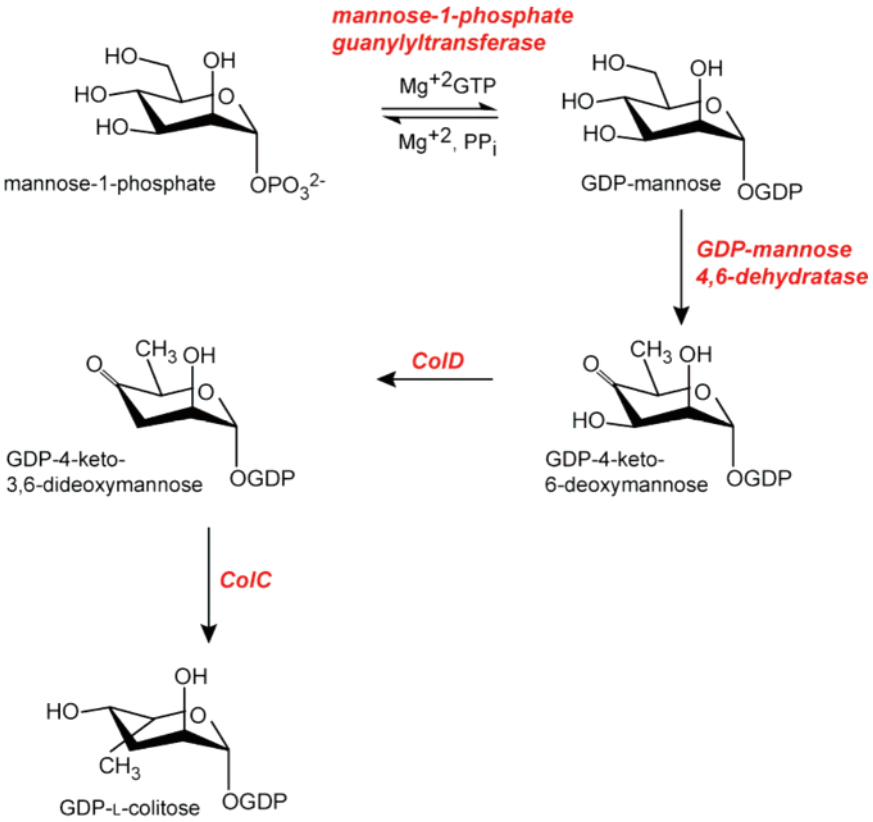

A perusal of any biochemistry textbook will attest to the fact that PLP is a remarkably versatile coenzyme found throughout nature. PLP-dependent enzymes catalyze an amazing repertoire of chemical reactions including decarboxylations, racemizations, transaminations, and eliminations, among others (*14*, *17*). Catalysis by these proteins is typically via a ping-pong mechanism whereby they oscillate between PLP- and PMP-bound forms. As noted above, most PLP-dependent enzymes contain an active site lysine, which forms a Schiff base with the coenzyme in the resting state. This species is known as the internal aldimine as indicated in Scheme 2. In many examples, the PLP cofactor is involved in transamination reactions, which typically begin when glutamate or another amino donor reacts with the internal aldimine. A transient geminal diamine is first formed (Scheme 2), which subsequently collapses to form a Schiff base between the cofactor and glutamate, referred to as the external aldimine.

A possible dehydration reaction mechanism for ColD, based on both biochemical and structural data, is presented in Scheme 3 (*13*, *18*). Consistent with all presently available data, it is thought that after the PLP has been converted to PMP, a Schiff base is then formed between the sugar C4′ and the PMP cofactor that is noncovalently bound to ColD. His 188 most likely serves as the catalytic base that initiates the deprotonation event leading to the intermediate labeled 2 in Scheme 3. The subsequent expulsion of the sugar C3′-hydroxyl group is facilitated by the now protonated form of His 188 which donates a proton to it. Following the departure of the hydroxyl group in the form of a water, a $\Delta^{3,4}$-aminomannoseen intermediate is generated (labeled 3 in Scheme 3). This intermediate is hydrolyzed by a water molecule that is activated by His 188, resulting in the intermediate labeled 4. The incorporation of a hydrogen at the sugar C3′ is believed to be catalyzed by the protonated form of His 188. Whether the final expulsion of ammonia, as indicated in Scheme 3, occurs in the enzyme active site or in solution is not known at the present time.

Recently, an elegant mechanistic study was conducted on an enzyme similar to ColD, CDP-6-deoxy-D-glycero-L-threo-4-hexulose-3-dehydratase (E_1). It catalyzes the removal of the sugar C3′-hydroxyl group in the biosynthesis of many CDP-linked 3,6-dideoxyhexoses (*19*). Although E_1 requires E_3 (with its accompanying cofactors) for activity, it is strikingly similar to ColD in that the typical active site lysine is replaced with a histidine. Interestingly, it was shown that changing this histidine in E_1 to a lysine residue via site-directed mutagenesis resulted in an enzyme with no dehydratase activity. The enzyme was, however, capable of performing a one-turnover event of the aminotransferase reaction (*19*).

In an effort to further probe the role of the active site histidine in ColD, a site-directed mutant protein was constructed whereby His 188 was replaced with a lysine. Here we present a combined structural and functional analysis of this protein from *Escherichia coli*, Strain 5a, type *O*55:H7. The structure reveals the geminal diamine intermediate trapped in the active site. In addition, functional assays demonstrate that this mutant form of ColD cannot catalyze the dehydration reaction leading to the removal of the C3′-hydroxyl group from the sugar moiety.

MATERIALS AND METHODS

Cloning, Site-Directed Mutagenesis, Expression, and Purification of ColD H188K. The gene encoding ColD was isolated as previously described (*13*) and used to produce

Scheme 2

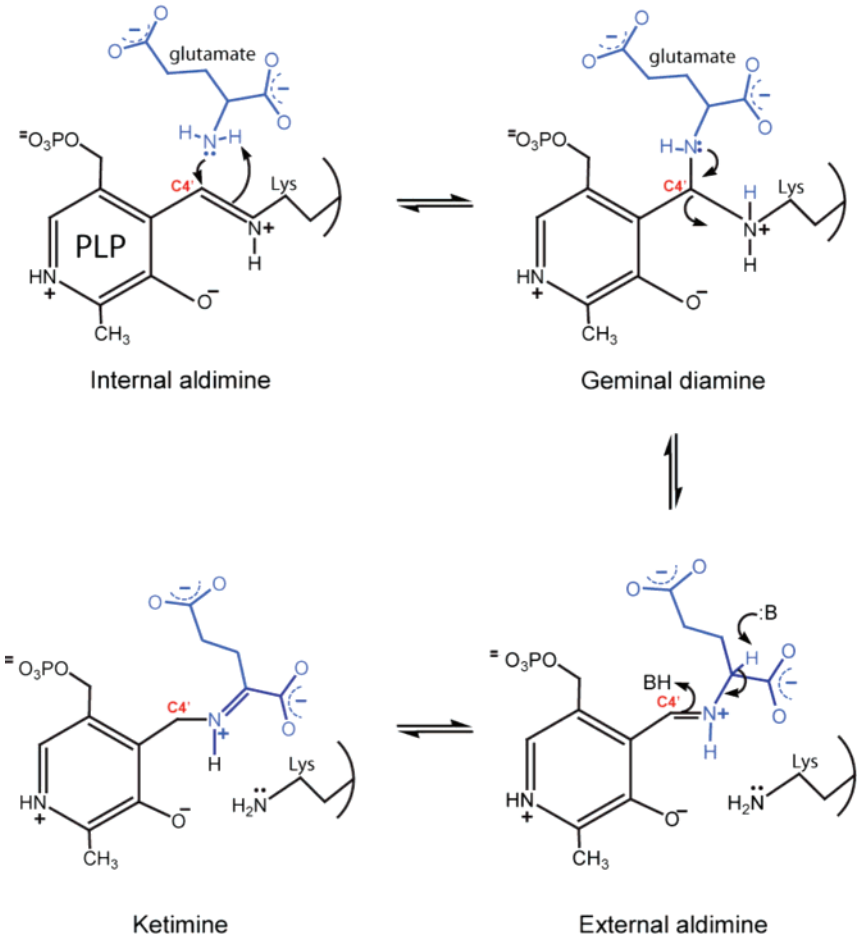

the ColD-pET28JT plasmid required for this investigation. His 188 was changed to a lysine through site-directed mutagenesis using the Quick Change Mutagensis Kit (Stratagene) with the following primer and its reverse complement: ggaacatttagctctttctattctaaacatatagctaccatgg. Mutagenesis was confirmed by DNA sequence analysis. The protein was expressed, purified, and digested with TEV protease as previously described (*13*). Subsequently, it was dialyzed against 25 mM Tris-HCl (pH 8.0) and 100 mM NaCl. Following dialysis, the sample was concentrated to 20 mg/mL as estimated by the absorbance at 280 nm using an extinction coefficient of 0.93 (mg/mL)$^{-1}$cm^{-1}, as determined by the ProtParam tool from the Expasy Proteomics Server. Wild-type enzyme required for the functional studies was expressed and purified as previously reported (*13*).

Crystallization of ColD H188K. Crystallization conditions were first surveyed by the hanging drop method of vapor diffusion using a sparse matrix screen developed in the laboratory. Large single crystals were subsequently grown via batch methods. The protein concentrations were typically 20 mg/mL, and the protein solutions were buffered with 25 mM Tris (pH 8.0) and contained 100 mM NaCl. The precipitant solutions were composed of 100 mM MES (pH 6.0), 24% poly(ethylene glycol) 3400, 600 mM KCl, 2 mM PLP, and 2 mM α-ketoglutarate. The crystals grew to maximum dimensions of 0.3 × 0.5 × 0.5 mm in ~30 days and belonged to the $P2_1$ space group with unit cell dimensions of a = 69.9 Å, b = 72.9 Å, c = 87.0 Å, and β = 107.9°. The asymmetric unit contained the complete ColD H188K dimer.

Single-Crystal UV/Visible Absorption Spectrum. ColD H188K crystals were transferred to a synthetic mother liquor consisting of 50 mM MES (pH 6.0), 30% poly(ethylene glycol) 3400, 400 mM KCl, and 2 mM α-ketoglutarate. The single-crystal spectrum was collected at the Kahlert Structural Biology Laboratory, University of Minnesota. The spectrum was recorded with a 4DX single-crystal microspectrophotometer (4DX, Sweden), equipped with an MS125TM 1/8m spectrograph (Thermo-Oriel, CT), a CCD detector (Andor Technology, UK), and a xenon lamp emitting from ~300 nm to above 800 nm (Zeiss,Germany). Data collection and analysis were performed using the Andor MCD software package (Andor Technology, UK) supplied with the CCD detector.

Aminotransferase Activity Assay. All required chemicals were purchased from Sigma. Solution UV/visible absorbance spectra were obtained for authentic samples of both PLP and PMP (data not shown). An absorbance peak at 395 nm with a 320 nm shoulder was observed for PLP whereas a single peak at 320 nm occurred for PMP. PLP and PMP were each run under the HPLC conditions stated below to determine their respective retention times (data not shown).

Incubations were conducted at room temperature in Buffer A (50 mM HEPES, pH 7.5, and 50 mM NaCl) with the addition of 25 mM glutamate, 0.5 μM PLP, and 10 μM enzyme for both the wild-type and the H188K ColD proteins. After 8 h, the reactions were boiled for 2 min to precipitate

Scheme 3

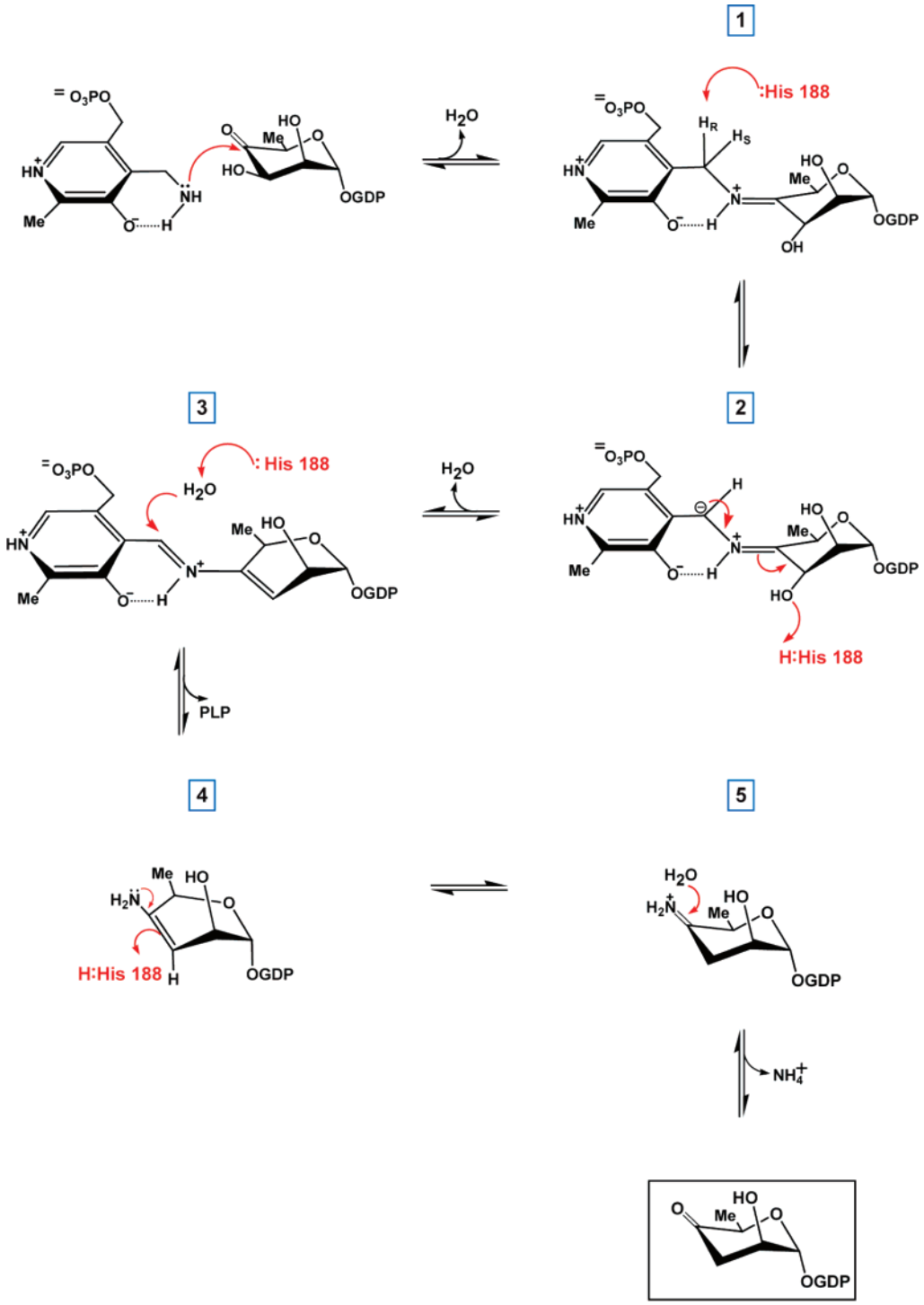

the protein, cooled on ice, and subsequently centrifuged at 12 000*g* for 2 min prior to removing the supernatant.

The presence of PLP and/or PMP was qualitatively determined by analyzing incubation mixture supernatants with an ÄKTA Purifier HPLC (Amersham-Pharmacia Biotech) equipped with a Resource-Q 1 mL anion exchange column (Amersham Biosciences). The column was equilibrated with Buffer A, after which 500 μL of the incubation supernatants were loaded and eluted with a linear gradient to 100% Buffer B (50 mM HEPES pH 7.5, 1M NaCl). The flow rate was 2 mL/min, and the elution was monitored at 320 and 395 nm.

Additionally, resting samples (500 μL of 2 μM) of both wild-type and mutant ColD proteins were heat denatured and run under identical conditions to determine if either cofactors were carried along during purification.

Dehydratase Activity Assay. The gene encoding GDP-mannose 4,6-dehydratase (Scheme 1) was isolated from *E. coli* O55:H7 as previously described (*20*), but a pET28JT vector (*13*) was used for protein expression. Purification was accomplished in one step with a Ni-NTA resin (Qiagen) according to the manufacturer's instructions. Typical ColD assay reactions contained 1 mM GDP-mannose, 2 mM glutamate, 0.2 mM PLP, 0.2 mM $NADP^+$, 3 μM GDP-

Table 1: X-ray Data Collection and Least-Squares Refinement Statistics

resolution limits (Å)	30−1.9
no. of independent reflections	60929 (7756)[b]
completeness (%)	93 (80)
redundancy	2.9 (1.2)
avg I/avg $\sigma(I)$	9.9 (1.6)
R_{sym} (%)[a]	6.3 (39.9)
R-factor (overall) %/no. of reflections[c]	18.5/60923
R-factor (working) %/no. of reflections	18.3/54920
R-factor (free) %/no. of reflections	25.5/6003
no. protein atoms[d]	6170
no. heteroatoms[e]	326
avg B values	
protein atoms (Å^2)	40.6
PLP derivatives (Å^2)	41.1
solvent (Å^2)	47.3
weighted root-mean-square deviations from ideality	
bond lengths (Å)	0.014
bond angles (deg)	2.0
trigonal planes (Å)	0.008
general planes (Å)	0.018
torsional angles (deg)[f]	18.3

[a] $R_{sym} = (\Sigma|I - \bar{I}|/\Sigma I) \times 100$. [b] Statistics for the highest resolution bin from 2.0−1.9 Å. [c] R-factor $= (\Sigma||F_o| - |F_c||/\Sigma|F_o|) \times 100$ where F_o is the observed structure-factor amplitude and F_c is the calculated structure-factor amplitude. [d] These include multiple conformations for Cys 197 in both subunits. [e] Heteroatoms include two PLP derivatives and 258 water molecules. [f] The torsional angles were not restrained during the refinement.

mannose 4,6-dehydratase, and 1 μM ColD in Buffer C (50 mM HEPPS, pH 8.0, and 50 mM NaCl). Reactions were incubated at room temperature for 2−4 h and boiled for 2 min to precipitate the protein. The samples were then cooled on ice and centrifuged at 12 000*g* for 2 min. Supernatants were removed and diluted 1:10 in water with 4% Buffer D (500 mM ammonium bicarbonate, pH 8.5).

ColD activity was qualitatively determined by analyzing reaction mixtures with mass spectrometry. The reactions were purified with an ÄKTA Purifier HPLC (Amersham-Pharmacia Biotech) fitted with a Resource-Q 1 mL anion exchange column (Amersham Biosciences). Diluted reactions were loaded onto the column and eluted with a linear gradient to 60% Buffer D. The flow rate was 2 mL/min, and the elution was monitored at 253 nm. Fractions from the peak corresponding to GDP-linked ketosugars (eluted at 185 mM ammonium bicarbonate) were pooled and freeze-dried using a Labconco 1L Freezone lyophilizer. Reaction contents were identified by ESI mass spectroscopy performed at the Mass Spectrometry/Proteomics Facility, University of Wisconsin−Madison.

Structural Analysis of ColD H188K. X-ray data were collected in-house at room temperature on a Bruker Proteum CCD detector system. The X-ray source was CuK_α radiation from a Rigaku RU200 X-ray generator operated at 50 kV and 90 mA. These data were processed with SAINT (Bruker AXS) and internally scaled with SADABS (Bruker AXS). Relevant X-ray data collection statistics are presented in Table 1.

The structure of ColD H188K was solved via molecular replacement with the program EPMR (*21*), employing the wild-type ColD structure (PDB accession no. 2GMU) as a search model with His 188, the cofactor, and all solvent molecules removed from the coordinate file (*13*). The initial R-factor was 30%. The model was subjected to least-squares refinement with the program TNT (*22*). Model building was done with the software package Coot (*23*). Relevant refinement statistics are given in Table 1.

RESULTS AND DISCUSSION

The structure of ColD H188K was solved to 1.9 Å resolution and refined to an overall R-factor of 18.5% for all measured X-ray data. Overall the electron densities corresponding to both subunits in the asymmetric unit were well-ordered except for the first two residues at the N-termini. Residues Met 193, Val 334, and Asn 354 in both subunits adopted ϕ, ψ angles lying outside of the allowed regions of the Ramachandran plot, specifically in the "nucleophile elbow" region. The electron densities for these residues were unambiguous, however, and the strained conformations for these residues were also observed in the wild-type structure (*13*). Other than these, the geometry of the model was excellent with 88.3%, 11.5%, and 0.1% of the remaining residues falling into the "most-favored," "additionally allowed" and "generously allowed" regions of the Ramachandran plot, respectively.

A ribbon representation of the ColD H188K dimer is presented in Figure 1a. As can be seen, the two subunits form a rather tight interface with a loop defined by Gln 235 to Glu 253 from one subunit curling over to complete the active site of the other subunit. This loop contains an α-helical turn defined by Gln 235 to Glu 238. Each subunit contains 13 α-helices and 13 strands of β-sheet. The two subunits of the dimer superimpose with a root-mean-square deviation of 0.27 Å for 376 structurally equivalent α-carbon positions. Since the electron density was somewhat better defined for Subunit 1, the following discussion will refer to it unless otherwise noted.

In the resting state of most PLP-dependent enzymes, the cofactor is covalently attached to the conserved lysine via a Schiff base (internal aldimine, Scheme 2). With this form, N^ζ of the lysine and C4′ of the cofactor are double-bonded and trigonal geometry is observed about both N^ζ and C4′. Upon forming PMP from PLP, a transient geminal diamine intermediate is produced in which both the glutamate and the lysine are bound to C4′ of the PLP cofactor. In this intermediate, the geometry about C4′ is tetrahedral, with single bonds connecting it to both the lysine N^ζ and the glutamate α-amino group. The next step occurs when the lysine N^ζ and C4′ bond breaks, leaving only the glutamate attached to the PLP cofactor. With this species, referred to as the external aldimine, there is a double bond between C4′ and the glutamate α-amino group, and the geometry about C4′ is trigonal planar (*24*).

We crystallized the ColD H188K protein in the presence of α-ketoglutarate and PLP in an attempt to observe the internal aldimine. A close-up view of the electron density corresponding to the H188K mutation is displayed in Figure 1b. To our surprise, as can be seen, the observed electron density was consistent with the formation of a geminal diamine intermediate which requires either the reaction of an internal aldimine with glutamate (Scheme 2) or α-ketoglutarate with PMP. Subsequent analysis of the α-ketoglutarate used in our crystallization trials revealed a contaminant peak in the mass spectrum that was consistent with glutamate.

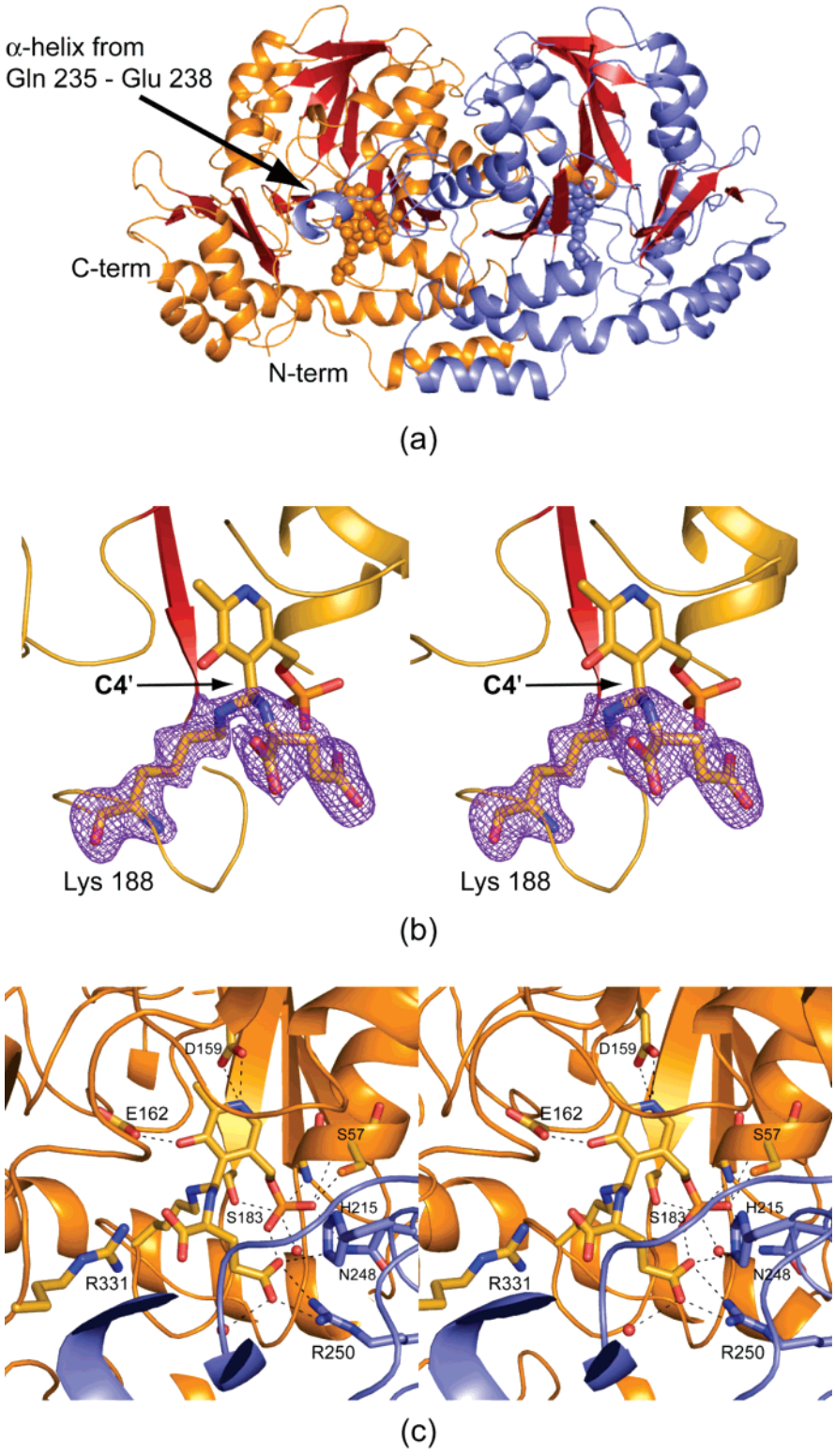

FIGURE 1: The structure of H188K ColD. (a) A ribbon representation of the dimeric protein with Subunits 1 and 2 color coded in gold and slate, respectively. The positions of the active sites are indicated by the space-filling representations for the geminal diamine intermediates. (b) Electron density corresponding to this intermediate in Subunit 1. The map was calculated with coefficients of the form ($F_o - F_c$), where F_o was the native structure factor amplitude and F_c was the calculated structure factor amplitude. Atoms corresponding to the intermediate and Lys 188 were excluded from the coordinate file during the least-squares refinement. The map was contoured at $\sim 3\sigma$. (c) A close-up view of the active site for Subunit 1. Those interactions between the intermediate and the protein, within 3.2 Å, are indicated by the dashed lines. Figures 1 and 3 were prepared with the software package PyMOL (*28*).

Even at a resolution of 1.9 Å, it is clear from the electron density that the geometry about the cofactor C4′ indicates sp^3 hybridization. While the UV/visible absorption data suggest that PMP and/or a PLP-glutamate ketimine intermediate may be present as well (as discussed further below), the electron density does not support the presence of either of these species at meaningful occupancies. Furthermore, if a mixture of the internal and external aldimines, the PMP cofactor, and/or the ketimine intermediate were present in the active site, an alternative conformation of the lysine

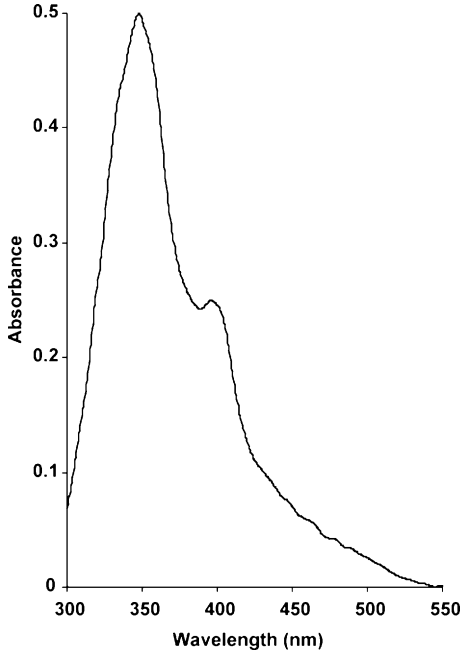

FIGURE 2: Single-crystal UV/visible absorption spectrum. The absorption spectrum from a ColD H188K single crystal shows two major peaks at 345 and 400 nm.

residue would be expected, given that it cannot be attached to C4′ if the external aldimine, the PMP cofactor, or the ketimine were present. In the structure described here, the lysine side chain is ~1.5 Å from C4′ of the PLP cofactor, indicating a carbon−nitrogen single bond. Attempts at modeling double bonds between C4′ and the lysine N^{ζ} or between C4′ and the glutamate α-amino group with appropriate sp^2 bond angles produced models that did not match the electron density well and, after refinement, caused positive and negative electron density peaks to appear in maps calculated with $(F_o - F_c)$ coefficients. Taken together, these X-ray crystallographic data strongly suggest that the electron density observed in the ColD H188K active site corresponds mostly to the geminal diamine intermediate.

To further verify the identity of this trapped intermediate, the UV/visible absorption spectrum was measured from a ColD H188K crystal grown in the same batch experiment as that utilized for X-ray data collection (Figure 2). This crystal demonstrated strong absorption at both 345 and 400 nm. PLP species known to absorb at 335−350 nm include the geminal diamine, the ketimine, the enolimine tautomers of the internal and external aldimines, and in some cases, PMP. The peak at 400 nm is most likely free PLP, either trapped within the crystalline lattice or present in the surrounding solution. The peak at 345 nm is somewhat asymmetric and may represent a convolution of several species. PMP, which typically absorbs at or slightly above 330 nm, may be present in the crystal. While the enolimine tautomers of the internal and external aldimines also absorb in this range, an absorption peak for the ketoenamine tautomers, which absorb at 420 nm, would also be expected (*25*). Therefore, the single-crystal UV/visible spectrum suggests that the crystal contains a convolution of species that possibly includes PMP, a PLP-glutamate ketimine intermediate, and the PLP-glutamate geminal diamine intermediate. Given the quality of the electron density, however, the geminal diamine intermediate is the most abundant species present. Although geminal diamines are exceedingly labile in solution, trapping them in the active sites of proteins belonging to the aspartate aminotransferase superfamily is not unprecedented. Indeed, such intermediates were first observed in the structural analysis at 2.9 Å resolution of mouse cytoplasmic serine hydroxymethyltransferase (*26*). A subsequent X-ray crystallographic investigation of rabbit cytoplasmic serine hydroxymethyltransferase at 2.8 Å resolution also revealed a geminal diamine intermediate (*27*).

A close-up view of the active site for ColD H188K is presented in Figure 1c. Similar to that observed for the wild-type enzyme, most of the protein:ligand interactions occur near the phosphoryl group of the cofactor. Specifically the side-chain groups of Ser 57 and Ser 183 from Subunit 1 and Asn 248 from Subunit 2 serve to anchor the phosphoryl oxygens into the active site. The backbone amide groups of Gly 56 and Ser 57 and an ordered water molecule provide additional hydrogen bonds to the phosphoryl oxygens. The side-chain carboxylate of the geminal diamine intermediate lies within 2.3 Å of a phosphoryl oxygen, indicating that one of these oxygens is protonated. In addition, this side-chain group forms an electrostatic interaction with the guanidinium moiety of Arg 250 from Subunit 2 and a

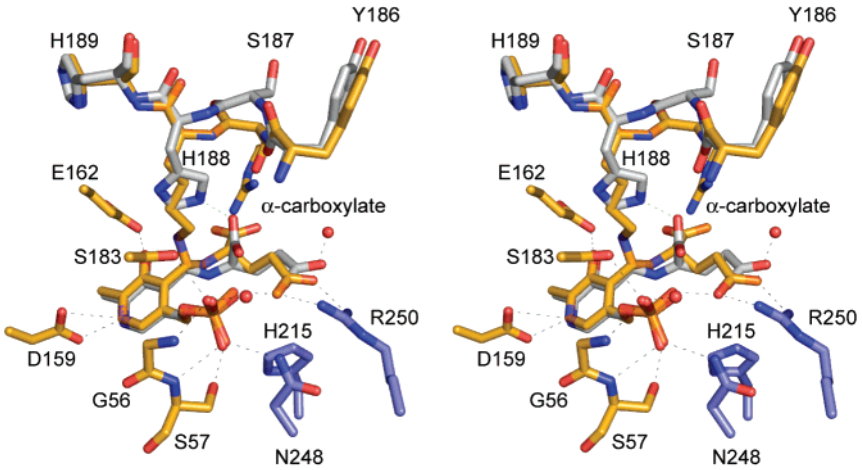

FIGURE 3: Superposition of the geminal diamine intermediate onto the ketimine intermediate. The model corresponding to ColD H188K is displayed in gold and slate bonds for Subunits 1 and 2, respectively. The positions of His 188 and the ketimine intermediate in the wild-type ColD model are highlighted in white bonds. Dashed lines indicate interactions within 3.2 Å of respective atoms.

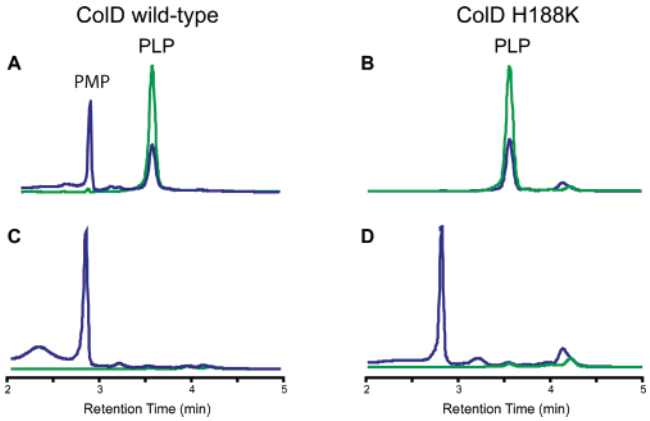

FIGURE 4: Formation of PMP by ColD. The elution was monitored at 320 nm (blue traces) and 395 nm (green traces). The resting form of wild-type ColD contains both PMP and PLP as indicated in Panel A. The resting form of ColD H188K contains only PLP (Panel B). When the enzyme in excess is incubated with PLP, near complete conversion of the PLP to PMP is observed for both the wild-type and mutant proteins as indicated in Panels C and D. The formation of PMP by the mutant protein can either be a result of true aminotransferase activity or a breakdown of the geminal diamine intermediate as a consequence of boiling.

hydrogen bond with an ordered water molecule. As observed in the wild-type structure, only two side chains, Asp 159 and Glu 162 form hydrogen bonds with the pyridoxal ring of the geminal diamine intermediate.

One significant difference between the wild-type and mutant protein structures occurs near the site of the mutation. The loop defined by Tyr 186 and His 189, which contains the H188K mutation, moves toward the geminal diamine intermediate (Figure 3). This shift is the result of a flip in the backbone ψ angle of Tyr 186 from 135° in the wild-type enzyme to −54° in the mutant protein. As a result of this flip, the position of the α-carbon of Ser 187 is shifted by 1.7 Å within the active site pocket and its side chain no longer points away but rather toward the PLP-derived cofactor. Conversely, the carbonyl oxygen of Tyr 186, which pointed toward the cofactor in the wild-type structure, is now positioned away from the cofactor in the mutant structure. Note that in the wild-type ColD/ketimine complex structure, the α-carboxylate group of the glutamate is situated near the imidazole group of His 188 whereas in the ColD H188K model this α-carboxylate shifts nearly perpendicular to its wild-type position and resides within 3.4 Å from the guanidinium group of Arg 331. It is possible that upon collapse of the geminal diamine intermediate, the α-carboxylate shifts to the position assumed in the wild-type enzyme for the ketimine intermediate.

To reiterate, the overall net reaction catalyzed by ColD is the removal of the C3′-hydroxyl group from the GDP-linked sugar. This involves a ping-pong catalytic mechanism in which PLP is first converted to PMP via its reaction with glutamate. The resulting PMP then reacts, as outlined in Scheme 3, with the C4′ sugar carbon to form a Schiff base. Shown in Figure 4 are the HPLC traces for the resting forms of the denatured wild-type (panel A) and mutant ColD (panel B) proteins. Note that pure samples of PMP and PLP have retention times of 2.8 and 3.6 min, respectively. Thus these traces demonstrate that wild-type ColD contains a mixture of both PLP and PMP, whereas the H188K mutant protein contains only PLP. To qualitatively determine if ColD

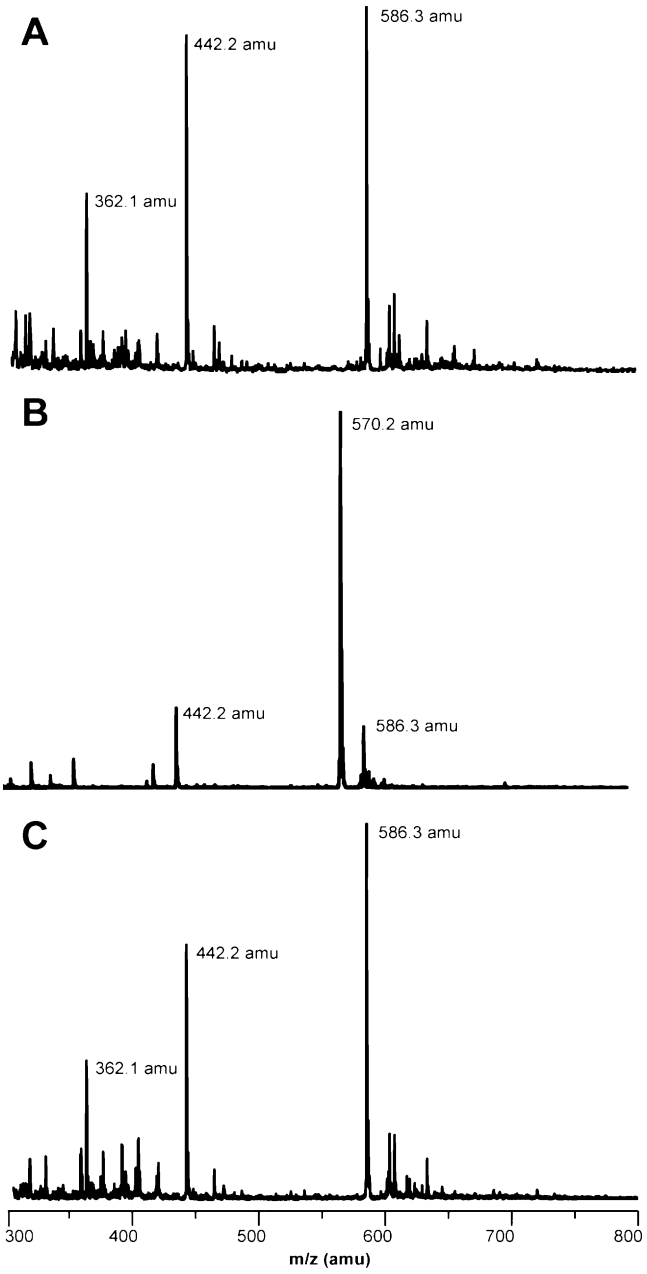

FIGURE 5: ESI mass spectra of wild-type and ColD H188K reactions. The spectrum of the reaction without the addition of ColD is given in Panel A and shows the buildup of GDP-4-keto-6-deoxymannose at 586.3 amu. Additional peaks at 442.2 and 362.1 amu result from the partial breakdown of this compound into GDP and GMP, respectively. The reactions with wild-type ColD given in Panel B show conversion of the 586.3 amu peak into a new peak at 570.2 amu, which is the appropriate mass of the ColD reaction product, GDP-4-keto-3,6-dideoxymannose. The reaction with ColD H188K shown in Panel C indicates a buildup of GDP-4-keto-6-deoxymannose and breakdown compounds.

H188K is capable of catalyzing the first half of the ping-pong mechanism, namely the transfer of an amino group, the following experiment was conducted. The concentration of enzyme was present in excess over that of PLP, and the glutamate was in a higher concentration than either the enzyme or the PLP cofactor. The HPLC traces displayed in Figure 4, panels C and D, indicate a complete conversion of PLP to PMP with both enzymes. A color change from yellow to colorless was observed during the incubation of both of these reactions, further suggesting that all PLP was

consumed. In the case of the wild-type enzyme, these data are consistent with complete conversion of PLP to PMP. With the mutant enzyme, two possible scenarios can be envisioned. Either the enzyme retains aminotransferase activity or the geminal diamine complex, as observed in the crystalline lattice, represents a dead-end complex, which breaks down to PMP because of the extreme conditions of the assay.

ESI mass spectrometry was used to ascertain whether H188K ColD retained any residual dehydratase activity. As shown in Figure 5, Panel A, the mass spectrum of the reaction of GDP-mannose with GDP-mannose 4,6-dehydratase (Scheme 1) without the addition of ColD resulted in the production of GDP-4-keto-6-deoxymannose at 586.3 amu. The additional peaks at 442.2 and 362.1 amu result from the partial breakdown of this compound into GDP and GMP, respectively. The mass spectrum of the reaction carried out in the presence of both the 4,6-dehydratase and wild-type ColD is shown in Figure 5, Panel B. In this situation, there is a conversion of the 586.3 amu peak into a new peak at 570.2 amu, which is the appropriate mass for the ColD reaction product, GDP-4-keto-3,6-dideoxymannose. There is no formation of GDP-4-keto-3,6-dideoxymannose when the reaction is carried out in the presence of ColD H188K (Figure 5, Panel C), thus indicating that the mutant protein is unable to catalyze the dehydration at the sugar C-3′. These activity results are similar to that observed for the histidine to lysine mutation of E_1, in which the dehydratase activity was abolished (*19*).

One of the fascinating questions regarding this mutant ColD protein is its inability to catalyze the dehydration step. One possibility is that it gets trapped as a dead-end geminal diamine complex because of the H188K mutation, and thus PMP is never formed which would prevent the dehydration step. If, however, the mutant protein is capable of converting PLP to PMP, then the inability to remove the C3′-hydroxyl group from the sugar moiety is probably a result of steric hindrance. The more bulky lysine side chain could prevent the proper positioning of the sugar group in the active site for effective catalysis. This issue will be more fully addressed when structures of ColD are solved in the presence of sugar substrates or analogues.

ACKNOWLEDGMENT

We thank Dr. Carrie Wilmot and Ms. Teresa De la Mora-Rey for help in obtaining the single-crystal UV/visible absorption spectrum. Special thanks go to Dr. James Thoden for his continued assistance throughout all stages of this investigation. We are indebted to Professor Rodney Welch for graciously providing genomic DNA, and we thank Professor Ivan Rayment for helpful discussions. The insightful comments of the reviewers are gratefully acknowledged.

REFERENCES

1. Rupprath, C., Schumacher, T., and Elling, L. (2005) Nucleotide deoxysugars: essential tools for the glycosylation engineering of novel bioactive compounds, *Curr. Med. Chem. 12*, 1637−1675.
2. Kennedy, J. F., and White, C. A. (1983) *Bioactive carbohydrates in chemistry, biochemistry and biology*, Ellis Horwood Publishers, Chichester, UK.
3. Lerouge, I., and Vanderleyden, J. (2002) *O*-antigen structural variation: mechanisms and possible roles in animal/plant-microbe interactions, *FEMS Microbiol. Rev. 26*, 17−47.
4. Luderitz, O., Staub, A. M., and Westphal, O. (1966) Immunochemistry of *O* and *R* antigens of *Salmonella* and related *Enterobacteriaceae*, *Bacteriol. Rev. 30*, 192−255.
5. Weymouth-Wilson, A. C. (1997) The role of carbohydrates in biologically active natural products, *Nat. Prod. Rep. 14*, 99−110.
6. Edstrom, R. D., and Heath, E. C. (1965) Isolation of colitose-containing oligosaccharides from the cell wall lipopolysaccharide of *Escherichia coli*, *Biochem. Biophys. Res. Commun. 21*, 638−643.
7. Kotandrova, N. A., Gorshkova, R. P., Zubkov, V. A., and Ovodov, Iu, S. (1989) The structure of the *O*-specific polysaccharide chain of the lipopolysaccharide of *Yersinia pseudotuberculosis* serovar VII, *Bioorg. Khim. 15*, 104−110.
8. Xiang, S. H., Haase, A. M., and Reeves, P. R. (1993) Variation of the *rfb* gene clusters in *Salmonella enterica*, *J. Bacteriol. 175*, 4877−4884.
9. Muldoon, J., Perepelov, A. V., Shashkov, A. S., Gorshkova, R. P., Nazarenko, E. L., Zubkov, V. A., Ivanova, E. P., Knirel, Y. A., and Savage, A. V. (2001) Structure of a colitose-containing *O*-specific polysaccharide of the marine bacterium *Pseudoalteromonas tetraodonis* IAM 14160(T), *Carbohydr. Res. 333*, 41−46.
10. Silipo, A., Molinaro, A., Nazarenko, E. L., Gorshkova, R. P., Ivanova, E. P., Lanzetta, R., and Parrilli, M. (2005) The *O*-chain structure from the LPS of marine halophilic bacterium *Pseudoalteromonas carrageenovora*-type strain IAM 12662T, *Carbohydr. Res. 340*, 2693−2697.
11. Bastin, D. A., and Reeves, P. R. (1995) Sequence and analysis of the *O* antigen gene (*rfb*) cluster of *Escherichia coli O*111, *Gene 164*, 17−23.
12. Beyer, N., Alam, J., Hallis, T. M., Guo, Z., and Liu, H. W. (2003) The biosynthesis of GDP-L-colitose: C-3 deoxygenation is catalyzed by a unique coenzyme B6-dependent enzyme, *J. Am. Chem. Soc. 125*, 5584−5585.
13. Cook, P. D., Thoden, J. B., and Holden, H. M. (2006) The structure of GDP-4-keto-6-deoxy-D-mannose-3-dehydratase: a unique coenzyme B_6-dependent enzyme, *Protein Sci. 15*, 2093−2106.
14. Jansonius, J. N. (1998) Structure, evolution and action of vitamin B_6-dependent enzymes, *Curr. Opin. Struct. Biol. 8*, 759−769.
15. Samuel, G., and Reeves, P. (2003) Biosynthesis of *O*-antigens: genes and pathways involved in nucleotide sugar precursor synthesis and *O*-antigen assembly, *Carbohydr. Res. 338*, 2503−2519.
16. Agnihotri, G., Liu, Y. N., Paschal, B. M., and Liu, H. W. (2004) Identification of an unusual [2Fe-2S]-binding motif in the CDP-6-deoxy-D-glycero-L-threo-4-hexulose-3-dehydrase from *Yersinia pseudotuberculosis*: implication for C-3 deoxygenation in the biosynthesis of 3,6-dideoxyhexoses, *Biochemistry 43*, 14265−14274.
17. Toney, M. D. (2005) Reaction specificity in pyridoxal phosphate enzymes, *Arch. Biochem. Biophys. 433*, 279−287.
18. Alam, J., Beyer, N., and Liu, H. W. (2004) Biosynthesis of colitose: expression, purification, and mechanistic characterization of GDP-4-keto-6-deoxy-D-mannose-3-dehydrase (ColD) and GDP-L-colitose synthase (ColC), *Biochemistry 43*, 16450−16460.
19. Wu, Q., Liu, Y. N., Chen, H., Molitor, E. J., and Liu, H. W. (2007) A retro-evolution study of CDP-6-deoxy-D-*glycero*-L-*threo*-4-hexulose-3-dehydrase (E1) from *Yersinia pseudotuberculosis*: implications for C-3 deoxygenation in the biosynthesis of 3,6-dideoxyhexoses, *Biochemistry 46*, 3759−3767.
20. Webb, N. A., Mulichak, A. M., Lam, J. S., Rocchetta, H. L., and Garavito, R. M. (2004) Crystal structure of a tetrameric GDP-d-mannose 4,6-dehydratase from a bacterial GDP-d-rhamnose biosynthetic pathway, *Protein Sci. 13*, 529−539.
21. Kissinger, C. R., Gehlhaar, D. K., and Fogel, D. B. (1999) Rapid automated molecular replacement by evolutionary search, *Acta Crystallogr. Sect. D: Biol. Crystallogr. 55 (Pt 2)*, 484−491.
22. Tronrud, D. E., Ten, Eyck, L. F., and Matthews, B. W. (1987) An efficient general-purpose least-squares refinement program for macromolecular structures, *Acta Crystallogr. Sect. D: Biol. Crystallogr. 43*, 489−501.

23. Emsley, P., and Cowtan, K. (2004) Coot: model-building tools for molecular graphics, *Acta Crystallogr. Sect. D: Biol. Crystallogr. 60*, 2126−2132.
24. John, R. A. (1995) Pyridoxal phosphate-dependent enzymes, *Biochim. Biophys. Acta 1248*, 81−96.
25. Malashkevich, V. N., Toney, M. D., and Jansonius, J. N. (1993) Crystal structures of true enzymatic reaction intermediates: aspartate and glutamate ketimines in aspartate aminotransferase, *Biochemistry 32*, 13451−13462.
26. Szebenyi, D. M., Liu, X., Kriksunov, I. A., Stover, P. J., and Thiel, D. J. (2000) Structure of a murine cytoplasmic serine hydroxymethyltransferase quinonoid ternary complex: evidence for asymmetric obligate dimers, *Biochemistry 39*, 13313−13323.
27. Scarsdale, J. N., Kazanina, G., Radaev, S., Schirch, V., and Wright, H. T. (1999) Crystal structure of rabbit cytosolic serine hydroxymethyltransferase at 2.8 Å resolution: mechanistic implications, *Biochemistry 38*, 8347−8358.
28. DeLano, W. L. (2003) *PyMOL Reference Manual*, DeLano Scientific LLC, San Carlos, CA.

BI701686S